

Crossover from paramagnetic compressed flux regime to diamagnetic pinned vortex lattice in a single crystal of cubic $\text{Ca}_3\text{Rh}_4\text{Sn}_{13}$

P. D. Kulkarni^{1,2}, S. S. Banerjee³, C. V. Tomy⁴, G. Balakrishnan⁵, D. McK. Paul⁵, S. Ramakrishnan¹ and A. K. Grover¹

¹*Department of Condensed Matter Physics and Materials Science,*

Tata Institute of Fundamental Research, Homi Bhabha Road, Colaba, Mumbai 400005, India.

²*Laboratorio de Bajas Temperaturas, Departamento de Fisica de la Materia Condensada, Instituto de Ciencia de Materiales Nicolas Cabrera, Universidad Autonoma de Madrid, 28049, Madrid, Spain*

³*Department of Physics, Indian Institute of Technology Kanpur, Kanpur 208016, India*

⁴*Department of Physics, Indian Institute of Technology Bombay, Mumbai 400076, India and*

⁵*Department of Physics, University of Warwick, Coventry CV4 7AL, United Kingdom*

(Dated: November 8, 2021)

We report the observation of positive magnetization on field cooling (PMFC) in low applied magnetic fields ($H < 100$ Oe) in a single crystal of $\text{Ca}_3\text{Rh}_4\text{Sn}_{13}$ near its superconducting transition temperature ($T_c \approx 8.35$ K). For $30 \text{ Oe} < H < 100 \text{ Oe}$, the PMFC response crosses over to a diamagnetic response as the temperature is lowered below 8 K. For $100 \text{ Oe} < H < 300 \text{ Oe}$, the diamagnetic response undergoes an unexpected reversal in its field dependence above a characteristic temperature (designated as $T_{VL}^* = 7.9$ K), where the field-cooled cool-down magnetization curves intersect. The in-phase and out-of-phase ac susceptibility data confirm the change in the superconducting state across T_{VL}^* . We ascribe the PMFC response to a compression of magnetic flux caused by the nucleation of superconductivity at the surface of the sample. In very low fields ($H < 20$ Oe), the PMFC response has an interesting oscillatory behaviour which persists up to about 7 K. The oscillatory nature underlines the interplay between competing responses contributing to the magnetization signal in PMFC regime. We believe that the (i) counterintuitive field dependence of the diamagnetic response for $H > 100$ Oe and above T_{VL}^* (lasting up to T_c), (ii) the oscillatory character in PMFC response at low fields and (iii) the PMFC peaks near 8.2 K in $30 \text{ Oe} \leq H \leq 100 \text{ Oe}$ provide support in favour of a theoretical scenario based on the Ginzburg-Landau equations. The scenario predicts the possibility of complex magnetic fluctuations associated with transformation between different metastable giant vortex states prior to transforming into the conventional vortex state as the sample is cooled below T_{VL}^* .

PACS numbers: 74.25.Ld, 74.25.Ha, 74.25.Op

I. INTRODUCTION

Superconducting specimens of different genre and with varying pinning have been known¹⁻¹⁰ to display an anomalous paramagnetic response, instead of the usual diamagnetic Meissner effect, on field-cooling in small magnetic fields (H). Such a response has been designated as the Paramagnetic Meissner Effect (PME) or the Wohleben effect¹, since the advent of superconductivity in cuprates. Originally this feature was found in granular^{2,3} form of the high T_c superconductor (HTSC) $\text{Bi}_2\text{Sr}_2\text{CaCu}_2\text{O}_8$ and in single crystals⁴ of $\text{YBa}_2\text{Cu}_3\text{O}_7$. Invoking the possible special d -wave symmetry of the superconducting order parameter in HTSC materials, different models, such as, the presence of an odd number of π -junctions in a loop leading to spontaneous circulating currents producing a positive magnetization signal, the presence of Josephson junctions (π - or 0 -), spontaneous supercurrents due to vortex fluctuations or an orbital glass^{5,6}, were proposed to explain the PME. However, the subsequent observation of positive magnetization even in conventional s -wave superconductors, like, moderately pinned Nb discs^{7,8}, nanostructured Al discs⁹ and a weakly pinned spherical single crystal¹⁰ of Nb, has indicated that the origin of positive magnetization on field cooling in these materials is perhaps related to flux trapping¹¹⁻¹⁴ and its possible subsequent compression^{11,13,14}.

Magnetic flux can get trapped in the bulk of a superconductor below T_c , as the preferential flux expulsion from the superconducting boundaries can lead to a flux free region near

the sample edges, which would grow as the sample is further cooled^{6,10-15}. In such a situation the magnetization response is governed by two counter flowing currents^{6,11}, a paramagnetic (pinning) current flowing in the interior of the sample, which is associated with the pinned compressed flux, and a diamagnetic shielding current flowing around the surface of the sample, which screens the flux free region near the sample surface from the externally applied fields. Since these currents flow in opposite directions, the resultant magnetization can either be positive or negative^{6,11,14}.

Attempts to understand PME via the Ginzburg-Landau (GL) equations have shown^{13,14} that a large compression of magnetic flux in the interior of the superconductor is energetically equivalent to the creation of giant vortex states, with multiple flux quanta $L\phi_0$, where the orbital quantum number, $L > 1$. Boundary effects in finite sized samples^{13,14,16} show that the Meissner state ($L = 0$ state) need not be the lowest energy state, but, a giant vortex state with $L > 0$ (in fact with $L > 1$) would have lower energy. Giant vortices are thus trapped inside the superconductor¹³ below a temperature where surface superconductivity¹⁵ is nucleated. Pinning may lead to a metastable giant vortex state with constant $L (> 1)$ getting sustained without decay into L states with lower energy¹³, as the temperature is gradually reduced. On approaching the bulk superconductivity regime, it is proposed theoretically¹⁴ that the transformation of a metastable giant vortex state into different lower L states can lead to a magnetization response having the tendency to fluctuate between

diamagnetic and paramagnetic values.

In an earlier work¹⁰, some of the present authors reported the observation of surface superconductivity¹⁵ concurrent with positive magnetization on field cooling (PMFC) (often designated as Paramagnetic Meissner Effect (see Ref. 6)) in a weak pinning spherical single crystal ($r_0 \approx 1.1$ mm) of Nb. However, there were no features in these experiments which could be ascribed to the metastable nature of giant vortex states in the temperature interval of the PMFC regime. In recent years, we have studied the ubiquitous Peak Effect (PE) phenomenon¹⁷ in single crystals of a large variety of low T_c and other novel superconductors^{18–22}. Amongst these, the cubic stannide, $\text{Ca}_3\text{Rh}_4\text{Sn}_{13}$ ($T_c \sim 8.35$ K)²¹, has a $\kappa \sim 18$. For this compound, we now present new and interesting results pertaining to the PMFC, emanating from the dc and ac magnetization measurements performed at low fields in close vicinity of T_c . The peak value of the paramagnetic signal in the field-cooled cool down (FCC) magnetization curves ($M_{FCC}(T)$) is inversely proportional to the magnetic field ($10 \text{ Oe} < H < 100 \text{ Oe}$) in which the sample is field-cooled. The paramagnetic signal close to T_c at very low fields ($H < 20 \text{ Oe}$) has a characteristic structure presenting a fluctuating response arising from competition between the paramagnetic and diamagnetic contributions. The ac susceptibility data also display interesting features, which appear consistent with the observations in dc magnetization measurements. A host of novel experimental findings reported here vividly illustrate the crossover from the compressed flux regime to the pinned conventional vortex lattice state, predicted and well documented by theorists in the literature^{6,13,14}.

II. EXPERIMENTAL DETAILS

The single crystals of $\text{Ca}_3\text{Rh}_4\text{Sn}_{13}$ were grown by the tin flux method²¹. Each growth cycle yielded a number of single crystals whose detailed pinning characteristics varied somewhat. The dc magnetization measurements were performed using a commercial SQUID-Vibrating Sample Magnetometer (Quantum Design (QD) Inc., USA, model S-VSM). In S-VSM, the sample executes a small vibration around a mean position, where the magnetic field is uniform and maximum. This avoids the possibility of the sample moving in an inhomogeneous field during the dc magnetization measurements. The remnant field of the superconducting magnet of S-VSM was estimated at different stages of the experiment, using a standard paramagnetic Palladium specimen. To ascertain the set value of the current supply energising the superconducting coil to yield nominal zero field at the sample position, we also relied on the identification of the change in sign of the z -component of the magnetic field on its gradual increase (1 to 2 Oe at a time) via independently examining the change in sign of the (field-cooled) magnetization values of the superconducting Sn specimen. The zero-field current-setting could thus be located to within ± 1 Oe in a given cycle of gradual change (increase or decrease) of field values from a given remnant state (positive or negative) of the superconducting magnet. The isofield temperature dependent magneti-

zation curves were recorded by ramping the temperatures in the range of 0.1 K/min to 0.5 K/min. The ac susceptibility measurements were carried out using another SQUID magnetometer (Q.D. Inc., USA, Model MPMS-5). The ac measurements were made at a frequency of 211 Hz and ac amplitude of 2.5 Oe (r.m.s.). The applied fields in dc and ac measurements were kept normal to the plane of the rectangular platelet (1 mm \times 2 mm \times 1.5 mm) shaped sample used in the present study.

III. RESULTS AND DISCUSSION

A. Peak effect characteristic in magnetic hysteresis (M - H) isotherms

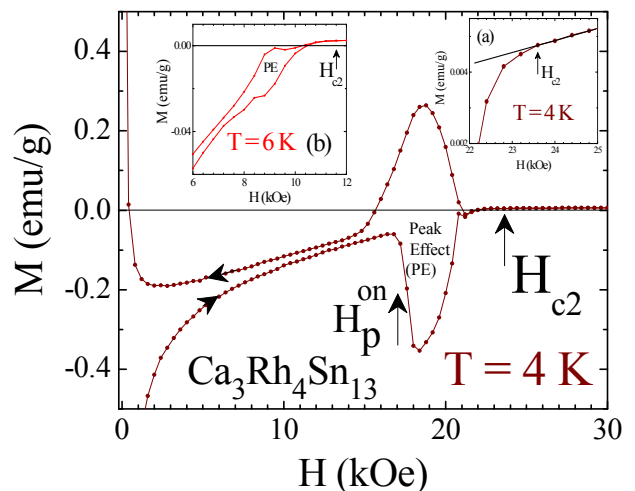


FIG. 1: (colour online) A portion of the dc magnetization hysteresis (M - H) curve at $T = 4$ K in a single crystal of $\text{Ca}_3\text{Rh}_4\text{Sn}_{13}$. The upper critical field (H_{c2}) and the onset field of the PE (H_p^{on}) are marked. Arrows on the curve indicate the directions of the field change. The inset (a) shows the expanded portion of M - H loop at 4 K to identify the onset of superconductivity at H_{c2} . The inset (b) shows an expanded portion of the M - H loop encompassing the PE region at 6 K.

The main panel of Fig. 1 shows a portion of the isothermal M vs H loop recorded at $T = 4$ K for a single crystal of $\text{Ca}_3\text{Rh}_4\text{Sn}_{13}$. The upper critical field (H_{c2}) and the onset field of the PE (H_p^{on}) are marked in the main panel. An anomalous enhancement of the magnetization hysteresis below H_{c2} is a fingerprint of the peak effect (PE) phenomenon in $\text{Ca}_3\text{Rh}_4\text{Sn}_{13}$ ¹⁹. The inset (a) in Fig. 1 elucidates the deviation from linearity nucleating at the paramagnetic-superconductor boundary, taken as H_{c2} . The inset (b) in Fig. 1 shows the PE region in a portion of the M vs H loop at 6 K, with H_{c2} marked as well. The second magnetization peak feature¹⁹ was not observed in the present sample. These data comprising only the PE attest to the high quality of the crystal^{19,21} chosen for our present study.

B. Positive magnetization close to the onset of superconductivity in isofield scans at low fields

An inset in Fig. 2 displays one of the typical temperature dependence of the $M_{FCC}(T)$ curves in low fields (viz., $H = 30$ Oe, here). M_{FCC} signal can be seen to saturate to its diamagnetic limit at low temperatures ($T < 6$ K). At the onset of the superconducting transition ($T_c = 8.35$ K), $M_{FCC}(T)$ response is, in fact, paramagnetic, which is evident in the plots of the expanded $M_{FCC}(T)$ curves for $H = 30$ Oe, 60 Oe and 90 Oe (see main panel of Fig. 2). The paramagnetic magnetization on field cooling (PMFC) in a given field ($H \leq 100$ Oe) reaches a peak value before turning around to crossover towards diamagnetic values (near 8 K). The PMFC data for $30 \text{ Oe} \leq H \leq 90 \text{ Oe}$ in Fig. 2 reveal that (i) the height of the paramagnetic peak decreases monotonically as H increases and (ii) the competition between positive signal and the diamagnetic shielding response gives rise to the turnaround behaviour in PMFC signals near 8.15 K. No significant difference was noted between PMFC response at $T > 8.2$ K for $H < 100$ Oe in the data recorded (not shown here) during the field-cooled warm-up (FCW) and FCC modes. This in turn implies that the positive magnetization signals above about 8.2 K do not depend on the thermomagnetic history of the applied magnetic field. This led us to explore closely the isothermal magnetization hysteresis loops in the temperature range $8 \text{ K} < T < 8.35 \text{ K}$.

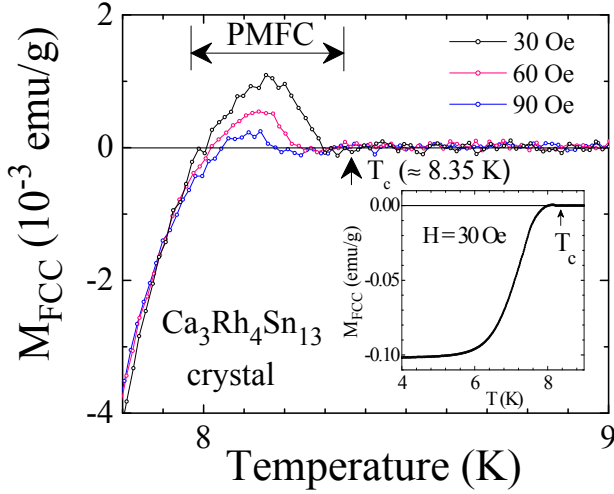


FIG. 2: (colour online) The inset panel shows the temperature variation of M_{FCC} in $H = 30$ Oe in a single crystal of $\text{Ca}_3\text{Rh}_4\text{Sn}_{13}$. The main panel shows portions of $M_{FCC}(T)$ curves at $H = 30$ Oe, 60 Oe and 90 Oe.

Figures 3(a) to 3(c) show the pair-wise plots of $M-H$ data recorded at 8.15 K, 8.20 K and 8.25 K in comparison with the corresponding data at 8.35 K. For each curve, the sample was cooled down to a given temperature in a field of +500 Oe. The field was then repeatedly ramped between ± 500 Oe. Note first that the $M-H$ data at 8.35 K is linear and passes through the origin, as anticipated, since this temperature identifies the onset of the superconducting transition ($T_c = 8.35$ K). The pair

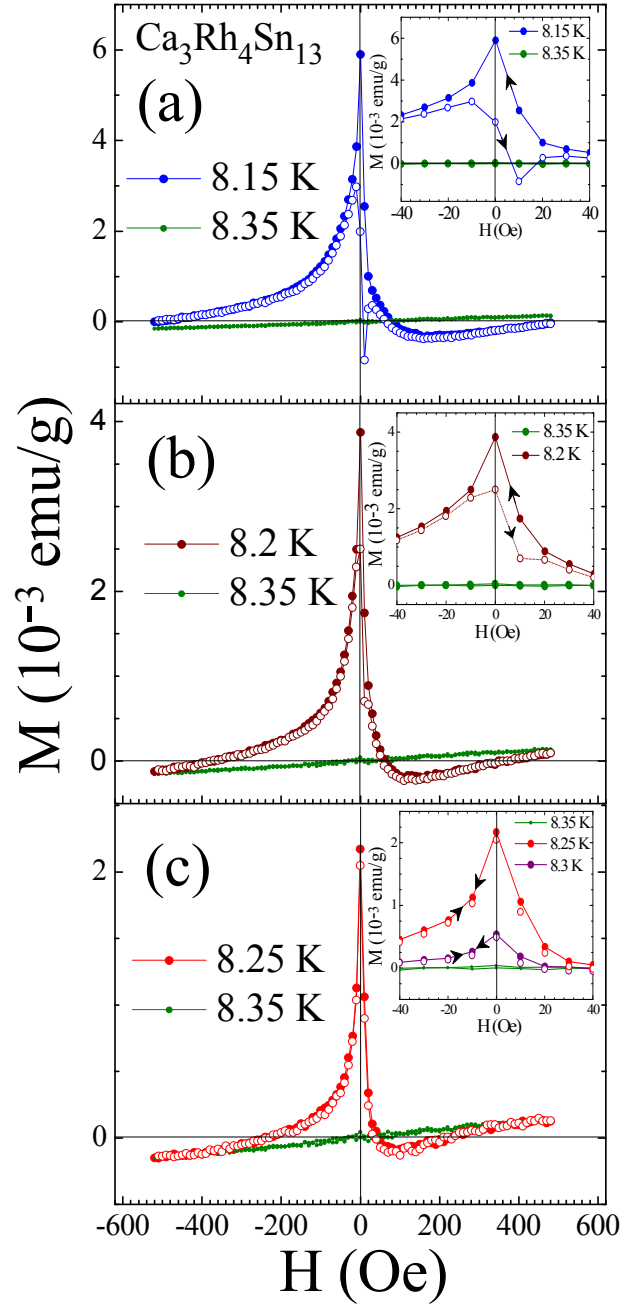


FIG. 3: (colour online) Magnetization vs applied magnetic field at (a) 8.15 K, (b) 8.2 K and (c) 8.25 K, in $\text{Ca}_3\text{Rh}_4\text{Sn}_{13}$. In each of the panels, M vs H plot at 8.35 K is also shown. The filled/open circles in each panel represent scans from $+/-500$ Oe to $-/+500$ Oe, respectively. Inset panels show the $M-H$ data across the zero field region on expanded scales.

of $M-H$ plots (at 8.25 K and 8.35 K) in Fig. 3(c) reveal that even at 8.25 K, a diamagnetic response (as determined by the difference between the two plots) is clearly present at about 250 Oe. On lowering the field below about 40 Oe, a sharp upturn takes the magnetization from diamagnetic to paramagnetic values. The paramagnetic response reaches its peak value at the zero applied field (in the z -direction). The peak

value of the paramagnetic signal in zero field is seen to decrease with enhancement in field on either side of the zero field. An inset in Fig. 3(c) shows a comparison of the field variation of the paramagnetic response at 8.25 K and 8.30 K on either side of the zero field on an expanded scale. Note the asymmetry in the field variation of the paramagnetic response at positive and negative fields. The observed asymmetry at 8.25 K and 8.3 K is independent of whether the sample is cooled first in +500 Oe or -500 Oe. We believe that the paramagnetic response at zero field (in z -direction), which is superconducting in origin, reflects the magnetization signal due to compression of field corresponding to x - and y -components of the earth's field. The magnetization value at zero field (in M - H loops) is found to be larger at 8.25 K as compared to that at 8.3 K (cf. inset in Fig. 3(c)). Such an enhancement characteristic can be seen to continue at a further lower temperature of 8.2 K (see inset panel of Fig. 3(b)). An inset panel in Fig. 3(a) shows the M - H plot at 8.15 K on the expanded scale across the zero-field region. From this inset panel, it is apparent that the M - H loop at 8.15 K has started to imbibe the characteristic of a hysteretic magnetic response in the neighbourhood of nominal zero field. The M - H loop at 8.15 K in the inset of Fig. 3(a), therefore, appears to be a superposition of (i) a hysteretic M - H loop expected in a type-II superconductor and (ii) a PMFC signal decreasing with enhancement in field on either side of the nominal zero-field.

The PMFC signal in $M(T)$ measurements in Fig. 2 for $\text{Ca}_3\text{Rh}_4\text{Sn}_{13}$ is an important observation at $H < 100$ Oe and $T > 8$ K. Above 100 Oe, the magnetization response in the superconducting state (at $T < 8.35$ K) is largely diamagnetic, however, an important unexpected change is witnessed in the field dependence of the diamagnetic response in the neighbourhood of 8 K, as described ahead.

C. Crossover from compressed flux regime to pinned vortex lattice regime below 8 K

The main panel in Fig. 4 displays the portions of the $M_{FCC}(T)$ curves close to T_c in $H = 100$ Oe, 200 Oe and 300 Oe in $\text{Ca}_3\text{Rh}_4\text{Sn}_{13}$. The most striking feature of these data is the intersection of the $M_{FCC}(T)$ curves at 7.9 K (identified as T_{VL}^*). Below T_{VL}^* , the magnitude of the diamagnetic response decreases as the field increases, as expected for the vortex lattice (VL) in a type-II superconductor. However, for $7.9 \text{ K} < T < 8.35 \text{ K}$, the magnitude of the diamagnetic response is enhanced as the field increases, which is unusual for a conventional low- T_c type-II superconductor. Such a behaviour, however, has been reported²³⁻²⁵ in the context of a high- T_c Josephson-coupled layered superconductor (JCLS) $\text{Bi}_2\text{Sr}_2\text{CaCu}_2\text{O}_{8-\delta}$ ($\text{Bi}2212$) for $H \parallel c$, where a crossover happens at a corresponding T^* value between the type-II response of a JCLS and the superconducting fluctuations-dominated response of the decoupled pancake vortices. In the case of $\text{Ca}_3\text{Rh}_4\text{Sn}_{13}$, the crossover at T_{VL}^* is, however, between the pinned vortex lattice state (VL) and the compressed flux regime, giving rise to PMFC signals at $H < 150$ Oe in the neighbourhood of T_c . We identify the region between T_c and

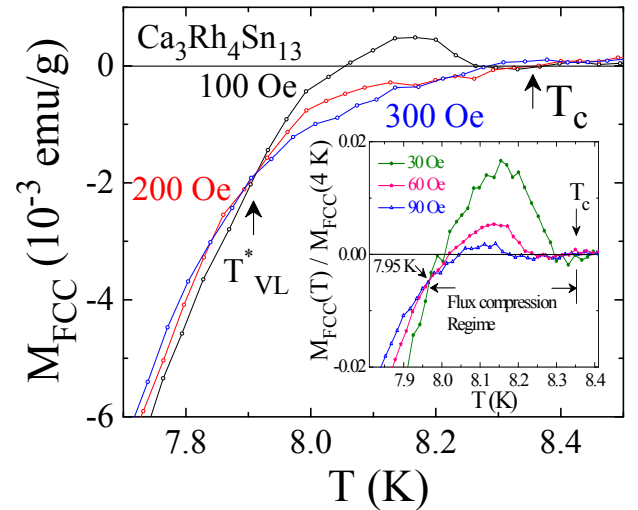


FIG. 4: (colour online) Portions of the field-cooled cool down magnetization as a function of temperature at $H = 100$ Oe, 200 Oe and 300 Oe in $\text{Ca}_3\text{Rh}_4\text{Sn}_{13}$. The transition temperature T_c and the temperature corresponding to the intersection of the three $M_{FCC}(T)$ curves (identified as T_{VL}^*) are marked in the main panel. The inset panel shows the temperature dependences of the normalized magnetization (see text) at lower fields, $H < 100$ Oe. The flux compression region has been identified in the temperature interval from T_c down to the crossover temperature.

T_{VL}^* as the flux compression region.

The $M_{FCC}(T)$ curves for $H < 100$ Oe, shown in Fig. 2, did not intersect at a unique temperature. However, if the $M_{FCC}(T)$ curves (for $30 \text{ Oe} \leq H \leq 90 \text{ Oe}$) are normalized to their respective values at 4 K, we observe a crossover at 7.95 K (see the inset panel of Fig. 4). Below 7.95 K, the response of the normalized $M_{FCC}(T)$ curves for different H is like that in a pinned type-II superconductor, and above 7.95 K, there exists the compressed flux regime^{11,13}, accounting for the positive peaks in magnetization above 8 K and up to T_c .

D. Oscillatory behaviour in field-cooled magnetization curves at low fields

Figure 5 summarizes the M_{FCC} data sequentially recorded from $H = -16$ Oe to $+14$ Oe in the single crystal of $\text{Ca}_3\text{Rh}_4\text{Sn}_{13}$. The sample was initially cooled in the remnant field of the superconducting magnet, whose value was estimated by measuring the paramagnetic magnetization of the standard Pd sample. The current in the superconducting coil was then incremented step-wise so as to enhance magnetic field by 2 Oe each time. The following characteristics are noteworthy in Fig. 5: (i) While in positive fields ($H \geq 2$ Oe), the PME signal close to T_c gives way to diamagnetic Meissner response at lower temperatures, in negative fields, the same PME signal close to T_c adds on to the positive Meissner response at lower temperatures. Thus, there is no change in the sign of magnetization response as a function of temperature in negative fields. The anomalous PME peak feature promi-

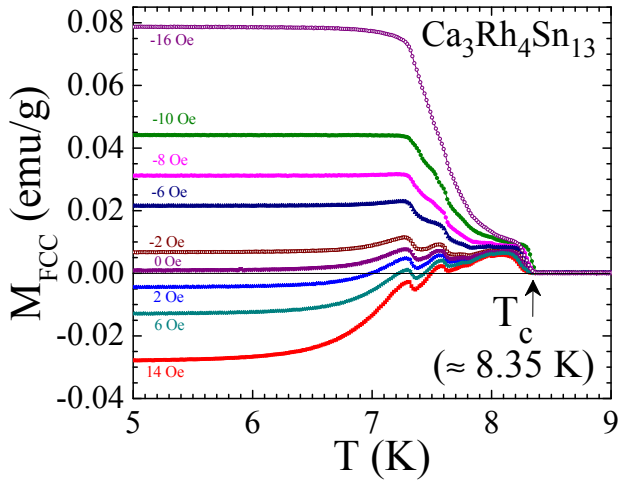


FIG. 5: (colour online) Temperature dependences of the field-cooled cool down magnetization ($M_{FCC}(T)$) values measured in $\text{Ca}_3\text{Rh}_4\text{Sn}_{13}$ by progressively incrementing the applied field from -16 Oe to $+14$ Oe.

nently evident at positive fields, therefore, takes the form of an onset of a sharper upturn in magnetization below 8 K in negative fields. (ii) A vivid oscillatory character is present below 8.2 K in the $M_{FCC}(T)$ curves for fields ranging from $H = -6$ Oe to $+14$ Oe. On the negative field side, the oscillatory feature tends to get obscured at $H = -10$ Oe. Details of the oscillatory structure between 8.2 K and 7 K depend somewhat on the rate of cooling down while recording the M_{FCC} data in a given field.

The asymmetry in response in the isofield runs in positive and negative fields ($|H| < 30$ Oe) in Fig. 5 correlates with the asymmetry in the response evident in $M-H$ isotherms shown in the inset panels of Fig. 3. The fact that the positive signal at nominal zero fields decays with field on either side of the zero-field (cf. plots at 8.25 K and 8.30 K in the inset of Fig. 3(c)) implies that the signal would not change sign in $M_{FCC}(T)$ curves measured for negative applied magnetic fields. For negative magnetic field, the diamagnetic shielding response emanating from a usual pinned type-II superconducting state would result in a positive signal in the magnetization measurements. Such a positive signal superposed on the PMFC magnetization signal (decaying with field) would rationalise the absence in the change of the sign of the PME signal in negative fields in temperature dependent scans.

Figure 6 shows a comparison of zero field-cooled (ZFC) magnetization response, $M_{ZFC}(T)$, in $H = 8$ Oe along with its $M_{FCC}(T)$ run. To record the $M_{ZFC}(T)$ run, the $\text{Ca}_3\text{Rh}_4\text{Sn}_{13}$ crystal was initially cooled down to 4 K (in estimated) zero field, the field was then incremented by $+8$ Oe and the magnetization was measured while slowly increasing the temperature above T_c . The crystal was then cooled down to 4 K to record the $M_{FCC}(T)$ data, and thereafter the magnetization was once again measured in the warm-up mode $M_{FCW}(T)$ to temperatures above T_c . The inset panel in Fig. 6 shows the plots of $M_{FCC}(T)$, $M_{FCW}(T)$ and $M_{ZFC}(T)$ close to T_c on an expanded scale. It can be noted that while the oscillatory

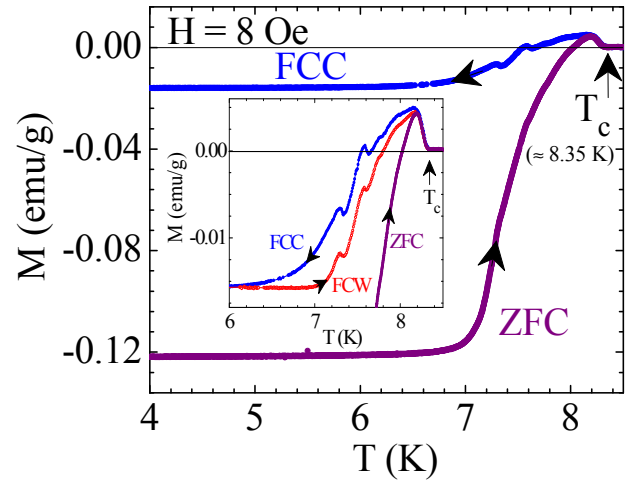


FIG. 6: (colour online) Temperature variation of the zero field-cooled (ZFC) and field-cooled (FC) dc magnetization curves in $H = +8$ Oe in $\text{Ca}_3\text{Rh}_4\text{Sn}_{13}$. The inset shows M_{ZFC} , M_{FCC} and M_{FCW} (field-cooled warm up) plots in $H = +8$ Oe on an expanded scale near T_c .

characteristic is evident in $M_{FCC}(T)$ and $M_{FCW}(T)$ runs, the $M_{ZFC}(T)$ is devoid of any oscillatory modulation feature as the diamagnetic response (in $+8$ Oe) crosses over to yield the attribute of PME peak between 8 K and 8.35 K. The three curves in the inset panel of Fig. 6 meet near 8.2 K, above which the path independent paramagnetic response monotonically decreases. It is reasonable to state that during the ZFC run in $H = 8$ Oe, the quantized vortices will enter the sample at a temperature at which the lower critical field $H_{c1}(T)$ becomes less than 8 Oe (ignoring the surface barrier effects). The quantized vortices will distribute inside the sample to yield Bean's Critical State²⁶ profile and the macroscopic currents $J_c(B)$ will flow inside the sample. The onset of sharp fall in $M_{ZFC}(T)$ above 7 K reflects the decrease in $J_c(B)$ with T on approaching the superconducting transition temperature.

It is tempting to associate the oscillatory responses in Fig. 5 to the notion of competition between the (Abrikosov) quantized vortices splitting out of the giant vortex state(s) in the form of compressed flux, and the tendency of a given giant vortex to retain (i.e., conserve) its angular momentum¹³ due to pinning. The high κ of $\text{Ca}_3\text{Rh}_4\text{Sn}_{13}$ ordains that the different L states of the giant vortex are closely spaced in energy. By lowering the temperature, there is a tendency to transform from $L > 1$ state to $L = 1$ state (Abrikosov state). However, theoretical work^{13,14} has shown that, due to pinning, the system can exhibit metastability, wherein, there can be fluctuations in magnetization corresponding to the transformation between different metastable L states before the system attains the $L = 1$ state.

In the framework of GL equations yielding multi-flux quanta, the magnetization due to different L states follow different temperature dependences at different reduced fields (i.e., applied field normalized to the thermodynamic critical field, H_c). In very low reduced fields (h) (e.g., $h \approx 0.001$, $\kappa \approx 10$ and cylindrical geometry), it has been calculated¹³ that all the L states will make paramagnetic contributions such that

higher L values contribute more. In the case of $\text{Ca}_3\text{Rh}_4\text{Sn}_{13}$, where $H_c \approx 3 \text{ kOe}$ ¹⁹, the PMFC response is observed in the range of reduced fields, 10^{-3} to 10^{-2} , where contributions from $L \geq 1$ states slightly below T_c could be paramagnetic. If the possible transitions between different high L states occur at the same temperature in the very low h range, one could rationalize the insensitivity of oscillatory pattern to the applied fields in Fig. 5. We may also add here that in the GL scenario, the irreversibility temperature is argued¹³ to correspond to a crossover between giant vortex states and the Abrikosov quantized vortices, consistent with the observations shown in Fig. 6.

The difference in the (diamagnetic) magnetization behaviour in FCC and FCW modes had been noted in samples of conventional low- T_c ²⁷ and high T_c ²⁸ superconductors. Clem and Hao²⁹ had shown how it could be rationalized in the framework of the Critical State Model²⁶. The spatial distribution of macroscopic currents ($J_c(B)$, where B is the local magnetic field) that are set up within an irreversible type-II superconductor while cooling down is different from that which emerges while warming up the sample in the same external field. The diamagnetic M_{FCW} curve typically lies below the M_{FCC} curve, and the two curves merge at the irreversibility temperature²⁹, where $J_c(B)$ vanishes. In high T_c superconductors the irreversibility line lies well below the H_{c2} line. In strongly pinned samples of type-II superconductors, the irreversibility temperature $T_{irr}(H)$ approaches $T_c(H)$ ³⁰. In this context, the merger of M_{FCW} and M_{FCC} curves in $H = 8 \text{ Oe}$ (cf. inset, Fig. 6) could imply that the macroscopic $J_c(B = 8 \text{ Oe})$ approaches zero just above 8.2 K. We may further add that the overlap of M_{FCC} and M_{FCW} curves at $T > 8.2 \text{ K}$ in Fig. 6 and the behaviour of M vs H at 8.25 K in Fig. 3(c) validates the theoretical prediction¹³ that the PMFC signal first decays rapidly with field, followed by the emergence of a diamagnetic response at higher fields.

E. AC susceptibility measurements in $\text{Ca}_3\text{Rh}_4\text{Sn}_{13}$

Figures 7 and 8 summarize the in-phase (χ') and out-of-phase (χ'') ac susceptibility data recorded in h_{ac} of 2.5 Oe (r.m.s.) iso-field and iso-thermal runs, respectively. The iso-field runs were made while cooling down from the normal state ($T > 8.35 \text{ K}$). The isothermal data were recorded along four or five quadrants within the field limits of $\pm 200 \text{ Oe}$, for the sample having been initially cooled in nominal zero field or + 500 Oe, respectively.

Figures 7(a) and 7(b) show the $\chi'(T)$ and $\chi''(T)$ plots recorded while cooling down the $\text{Ca}_3\text{Rh}_4\text{Sn}_{13}$ crystal in dc fields of 0 Oe (nominal value), 10 Oe, 30 Oe, 60 Oe and 90 Oe, respectively. The T_c and T_{VL}^* values stand marked appropriately in these two panels. The χ' response below as well as above T_{VL}^* remains diamagnetic. However, a conspicuous change in temperature dependence of χ' can be noted to happen near T_{VL}^* . Such a change is often ascribed¹⁰ to the crossover between the shielding response in the bulk to the shielding response from the surface superconductivity. In the present case, where we witness the PMFC signal above 8 K in

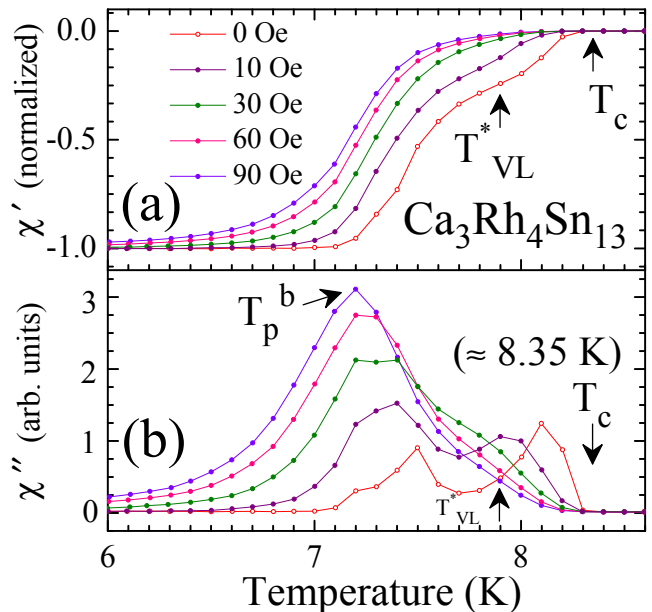


FIG. 7: (colour online) Panels (a) and (b), respectively, show the temperature variation of the in-phase (χ') and out-of-phase (χ'') ac susceptibility in $\text{Ca}_3\text{Rh}_4\text{Sn}_{13}$ at different fields, as indicated.

dc magnetization data, it can be noted that $\Delta M/\Delta H$ is negative (cf. Fig. 4), which rationalizes the diamagnetic χ' response above T_{VL}^* in Fig. 7(a).

The $\chi''(T)$ data in Fig. 7(b) shows a dissipation response measured with an ac amplitude of 2.5 Oe (r.m.s.) on either side of T_{VL}^* of 7.9 K. The two peaks of $\chi''(T)$ curve in nominal zero dc field in Fig. 7(b) support the notion of a crossover from superconductivity in the bulk (below 7.9 K) to the compressed flux regime (above it). The peak intensity of the higher temperature peak (above 7.9 K) diminishes as the field increases from 10 Oe to 60 Oe. This correlates with the decline in the paramagnetic response with enhancement in field in the temperature regime of compressed magnetic flux (cf. Fig. 2 and Fig. 3(c)). A comparison of $\chi''(T)$ curves from $H = 0 \text{ Oe}$ to 90 Oe below 7.9 K reveals that the lower temperature dissipative peak progressively becomes more prominent and the peak temperature moves inwards with the enhancement in dc field. This is the usual behaviour expected for enhanced irreversibility on cooling due to macroscopic currents set up within the bulk of a pinned type-II superconductor. The field (H) dependence of the peak temperature (T_p^b) of the dissipative peak below 7.9 K can easily be rationalized in terms of field/temperature dependence of macroscopic currents ($J_c(B, T)$), flowing as per Critical State Model²⁶ in the bulk of the sample.

Hysteretic behaviour in isothermal $\chi'(H)$ and $\chi''(H)$ were present at the $T > 7.5 \text{ K}$, however, the qualitative feature in field dependence of $\chi'(H)$ and $\chi''(H)$ during field ramp-up or ramp-down remained the same. Above 8 K, $\chi'(H)$ and $\chi''(H)$ data did not display significant hysteresis. To facilitate the comparison with the dc magnetization data in Fig. 3, we show in Figs. 8(a) to 8(d) the χ' vs H and χ'' vs H data recorded

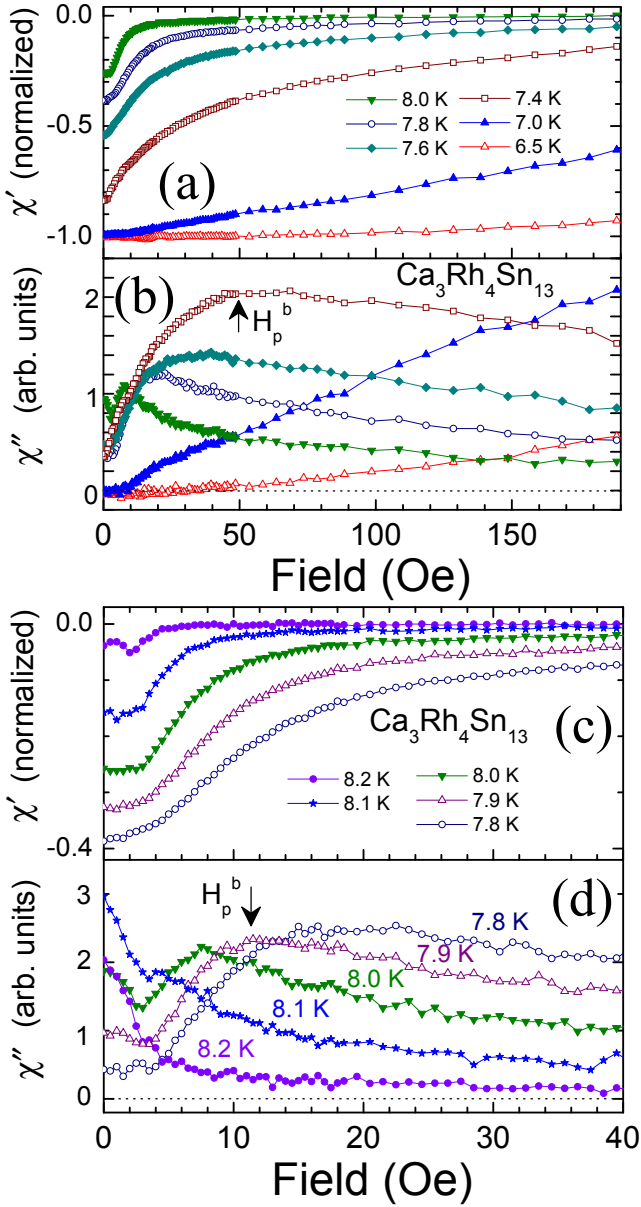


FIG. 8: (colour online) Panels (a) and (b), respectively, show the field variation of the in-phase (χ') and out-of-phase (χ'') ac susceptibility in $\text{Ca}_3\text{Rh}_4\text{Sn}_{13}$ at the temperatures as indicated. Panels (c) and (d), respectively, show the field dependence of χ' and χ'' at selected temperatures on going across T_{VL}^* .

at selected temperatures below and above T_{VL}^* of 7.9 K for field ramp down from +200 Oe to 0 Oe, for sample having cooled in +500 Oe. The $\chi'(H)$ response at 6.5 K in Fig. 8(a) shows that the given h_{ac} is almost completely shielded up to a dc field of 200 Oe. On raising the temperature to 7.0 K, the decline in $|\chi'|$ vs H in Fig. 8(a) reflects the field dependence of $J_c(B)$ at that temperature. The same trend continues on raising the temperature upto about 8.0 K. The χ'' vs H response at $T = 6.5$ K in Fig. 8(b) confirms that the h_{ac} of 2.5 Oe is not able to yield appreciable dissipation inside the sample upto a dc field of 200 Oe. However, χ'' vs H response at 7.0 K clearly

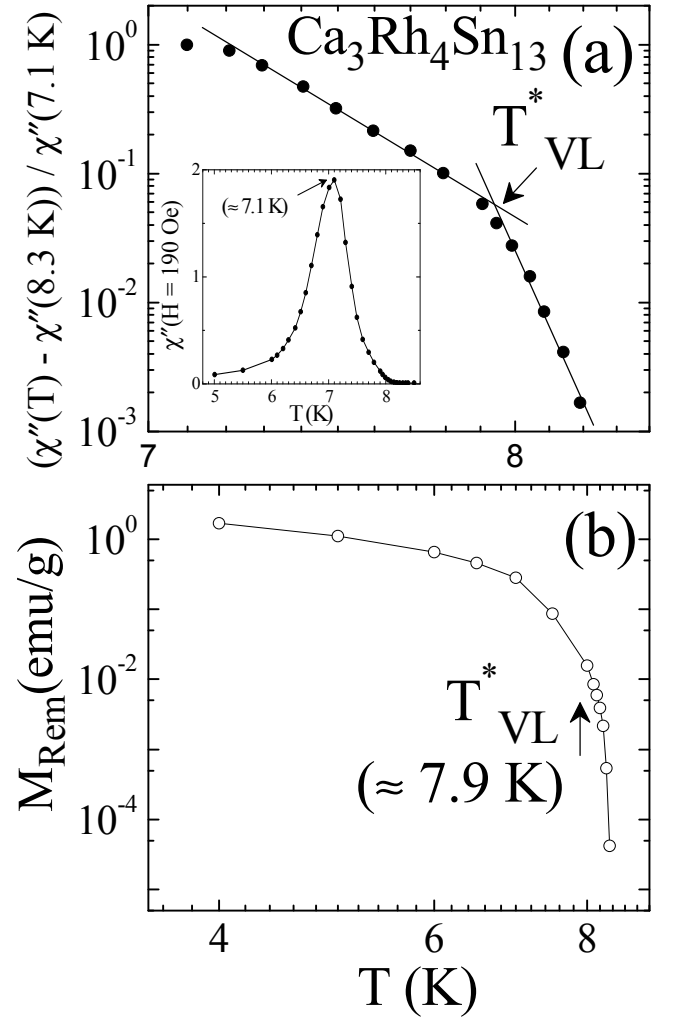


FIG. 9: Inset in panel (a) shows χ'' (at $H = 190$ Oe) as a function of temperature in $\text{Ca}_3\text{Rh}_4\text{Sn}_{13}$ showing the peak temperature at 7.1 K. Panel (a) shows temperature variation of the normalized χ'' (see text) and panel (b) shows M_{rem} values estimated from the dc magnetization loops like those given in Fig. 3.

reveals the presence of dissipative peak at a dc field of about 50 Oe (marked as H_p^b). Thereafter, the decrease in χ'' vs H reflects the field dependence of $J_c(B)$.

A very interesting behaviour in χ'' vs H , however, emerges (see Fig. 8(d)) as the temperature is raised from 7.8 K upto 8.1 K and beyond. The χ' vs H response at $T \geq 8.0$ K in Fig. 8(c) indicates that for the given h_{ac} , χ' has somewhat feeble field dependence at very low dc field ($H < 5$ Oe). The χ'' vs H curves in Fig. 8(d), however, reveal that a qualitative change in very low field ($H < 5$ Oe) response occurs at temperatures above 7.9 K. Note that χ'' vs H curves at 8.1 K and 8.2 K in Fig. 8(d) show the dissipation is maximum at nominal zero field, and it decreases rapidly on enhancing the dc field. The χ'' vs H curve at 8.0 K in Fig. 8(d) can be seen to imbibe the feature of a rapid decline of dissipation (which is maximum at zero field) with field, followed by surfacing of the dissipation peak (at H_p^b) due to currents in the bulk of

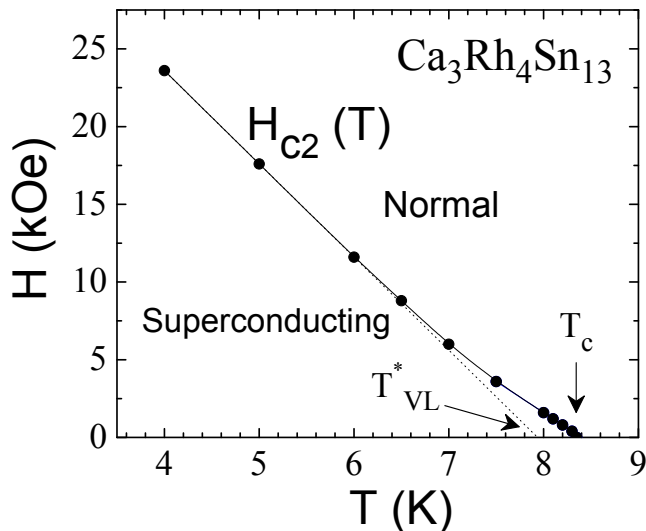


FIG. 10: The (H, T) phase diagram in a single crystal of $\text{Ca}_3\text{Rh}_4\text{Sn}_{13}$. The dashed line represents linear extrapolation of $H_{c2}(T)$ data. The temperature T_{VL}^* is marked at 7.9 K using the data in Fig. 2.

the sample. The data in Fig. 8(d), therefore, illustrate once again the crossover from a pinned type-II superconducting state to the compressed flux regime across the temperature region of about 8 K. The enhanced dissipation near zero field above 8.1 K perhaps indicates the dissipation from giant vortex cores with large L nucleated by surface superconductivity, whose evidence we have already shown in Fig. 7(b).

The inset of Fig. 9(a) shows a plot of χ'' vs T measured with an h_{ac} of 2.5 Oe (r.m.s.) in a dc field of 190 Oe. The observation of a peak in $\chi''(T)$ at 7.1 K implies that the given h_{ac} fully penetrates the bulk of the sample at this temperature in $H_{dc} = 190$ Oe. The decrease in $\chi''(T)$ above 7.1 K reflects the usual decrease in J_c with an increase in T . One can use this information to compute a relative dissipative response at $H = 190$ Oe w.r.t. the dissipation at the same field close the normal state, i.e., at 8.3 K $[(\chi''(T) - \chi''(8.3 \text{ K})) / \chi''(7.1 \text{ K})]$. This, in turn, amounts to computing the relative values of J_c in a field of 190 Oe w.r.t. its value at 7.1 K. The main panel of Fig. 9(a) shows a plot of the above stated relative response as a function of temperature. Note a change in the slope of the plotted curve at about 7.9 K (the so called T_{VL}^* value). We believe that the region beyond 7.9 K identifies the temperature dependence of surface pinning.

We have also plotted the remnant magnetization (or peak magnetization in close vicinity of the nominal zero field) determined from the $M-H$ loops (as in Fig. 3) as a function of temperature in Fig. 9(b). Such a remnant value (M_{rem}) could be taken as indicative of overall pinning in the specimen. We have marked the location of T_{VL}^* ($= 7.9$ K) in the semi-log plot of M_{rem} vs T in Fig. 9(b) to focus attention onto setting in of more rapid decline in $M_{rem}(T)$ on going across from (irreversible) pinned vortex lattice to paramagnetic compressed flux regime, where the remnant signal provides a measure of the dominance of the paramagnetic current.

IV. SUMMARY AND CONCLUSION

We have presented the results of dc and ac magnetization measurements at low fields in a weakly pinned single crystal of a low T_c superconductor, $\text{Ca}_3\text{Rh}_4\text{Sn}_{13}$, which crystallizes in a cubic structure. This system had been in focus earlier¹⁹ for the study of the order-disorder transformation in vortex matter (at $H > 3$ kOe) via the peak effect phenomenon. New results at very low fields and in close proximity of T_c have revealed the presence of positive dc magnetization on field cooling. In $H < 20$ Oe, PMFC signals nucleating at 8.35 K can be seen to survive down to about 7 K. For $30 \text{ Oe} < H < 100 \text{ Oe}$, the crossover from paramagnetic magnetization values to diamagnetic values is seen to occur near 8 K. For $100 \text{ Oe} \leq H \leq 300 \text{ Oe}$, the field cooled magnetization curves are observed to intersect at a temperature of 7.9 K, below which the diamagnetic response is akin to that expected for a pinned vortex lattice in a type-II superconductor. We have attributed the PMFC response to the notion of compressed flux trapped within the body of the superconductor. Below 20 Oe, the surfacing of a curious oscillatory structure in the PMFC response prompted us to invoke the possible notion of a conservation of angular momentum for the giant vortex state^{13,14} to account for this behaviour. The iso-field and iso-thermal ac susceptibility (χ' and χ'') data also seem to register the occurrence of a crossover between the compressed flux regime and the pinned vortex lattice.

To conclude, we show in Fig. 10 the plot of H_{c2} values as a function of temperature in the form of a magnetic phase diagram in which the normal and superconducting regions are identified. Between 4 K and 7 K, H_{c2} versus T has a linear variation; on extrapolation, this linear behaviour fortuitously meets the T -axis (where $H = 0$) at T_{VL}^* of 7.9 K. For $H < 300$ Oe, the fingerprints of a compressed flux regime in the form of PMFC and/or anomalous diamagnetic response ($\Delta M / \Delta H < 0$) can be observed between T_c and T_{VL}^* of 7.9 K. The region between $H_{c2}(T)$ line and the dotted line which meets the temperature axis at T_{VL}^* in Fig. 10 is the regime where we have identified the presence of surface superconductivity and surface pinning (cf. Fig. 9). If this were so, then the portion of $H_{c2}(T)$ which deviates from the extrapolated dotted line in Fig. 10, should be identified as a portion of the $H_{c3}(T)$ line. At somewhat below T_{VL}^* (e.g., at $T = 7.7$ K), an estimate of the ratio of fields associated with the dotted portion of the line and that of the $H_{c2}(T)$ line gives a value of about 2 which is more like the ratio of $H_{c3}(T) / H_{c2}(T)$. In a spherical single crystal of elemental Nb, whose κ value (~ 2) was just above the threshold for type-II response, some of us had reported¹⁰ the observation of surface superconductivity concurrent with the PMFC response over a large (H, T) domain, such that the $H_{c3}(T)$ was distinctly different from $H_{c2}(T)$ line in its phase diagram (Fig. 4 in Ref. 10). In the present case of $\text{Ca}_3\text{Rh}_4\text{Sn}_{13}$, where κ is large (~ 18), the PMFC signal, presumably sustained by the nucleation of superconductivity at the surface, is present only at low fields and in the close proximity to T_c . A sharp distinction between H_{c3} and H_{c2} is not discernible near T_c , the surface superconductivity could, however, be responsible for the slight concave curvature of the

$H_{c2}(T)$ curve near T_c in the magnetic phase diagram (cf. Fig. 10).

We believe that behaviour reported above in $\text{Ca}_3\text{Rh}_4\text{Sn}_{13}$ is generic. Similar features (In particular, an apparent absence of PME peak like feature in negative applied fields and the associated asymmetry between responses in positive/negative fields) would be present in other weak pinning superconductors. Preliminary searches in single crystal samples of other

superconducting compounds, like, $\text{Yb}_3\text{Rh}_4\text{Sn}_{13}$, NbS_2 , etc. have yielded positive indications³¹.

The single crystals grown at University of Warwick form a part of the continuing programme supported by EPSRC of U.K. We thank Mahesh Chandran for fruitful discussions. SSB would like to acknowledge the funding from Indo-Spain Joint Programme of co-operation in S & T, DST, India.

-
- ¹ D. I. Khomskii, *J. Low Temp. Phys.* 95, 205 (1994).
² W. Braunisch, N. Knauf, V. Kataev, S. Neuhausen, A. Grutz, A. Kock, B. Roden, D. Khomskii, and D. Wohlleben, *Phys. Rev. Lett.* 68, 1908 (1992); W. Braunisch, N. Knauf, G. Bauer, A. Kock, A. Becker, B. Freitag, A. Grutz, V. Kataev, S. Neuhausen, B. Roden, D. Khomskii, and D. Wohlleben, *Phys. Rev. B* 48, 4030 (1993); M. Sigrist and T. M. Rice, *J. Phys. Soc. Jpn.* 61, 4283 (1992).
³ P. Svedlindh *et al.* *Physica C* 162, 1365 (1989); B. Schliege *et al.* *Phys. Rev. B* 47, 8331 (1993); Ch. Heinzel *et al.* *Phys. Rev. B* 48, 3445 (1993); S. Elschner *et al.* *Supercond. Sci. Technol.* 6, 413 (1993); J. Magnusson *et al.* *Phys. Rev. B* 52, 7675 (1995).
⁴ S. Reidling *et al.*, *Phys. Rev. B* 49, 13283 (1994).
⁵ M. Sigrist, T.M. Rice, *Rev. Mod. Phys.* 67, 503 (1995) and references therein.
⁶ Mai Suan Li, *Physics Reports* 376, 133 (2003) and references therein.
⁷ D.J. Thompson, M.S.M. Minhaj, L.E. Wenger, and J.T. Chen, *Phys. Rev. Lett.* 75, 529 (1995); P. Kostic *et al.*, *Phys. Rev. B* 53, 791 (1996).
⁸ L. Pust, L. E. Wenger, and M. R. Koblischka, *Phys. Rev. B* 58, 14191 (1998).
⁹ A.K. Geim, S.V. Dubonos, J.G.S. Lok, M. Henini, and J.C. Maan, *Nature* 396, 144 (1998).
¹⁰ Pradip Das, C. V. Tomy, S. S. Banerjee, H. Takeya, S. Ramakrishnan, and A. K. Grover, *Phys. Rev. B* 78, 214504 (2008)
¹¹ A.E. Koshelev and A.I. Larkin, *Phys. Rev. B* 52, 13559 (1995).
¹² A.E. Khalil, *Phys. Rev. B* 55, 6625 (1997); M. Chandran, *Phys. Rev. B* 56, 6169 (1997).
¹³ V.V. Moshchalkov, X.G. Qui, and V. Bruyndoncz, *Phys. Rev. B* 55, 11793 (1995).
¹⁴ G. F. Zharkov, *Phys. Rev. B* 63, 214502 (2001).
¹⁵ D. Saint-James and P. G. de Gennes, *Phys. Lett.* 7, 306 (1963).
¹⁶ H. J. Fink and A. G. Presson, *Phys. Rev.* 151, 219 (1966).
¹⁷ A. B. Pippard, *Philos. Mag.* 19, 217 (1969); A. J. Larkin and Yu. M. Ovchinnikov, *J. Low. Temp. Phys.* 34, 409 (1979); G. Blatter, V. B. Geshkenbein, and J. A. G. Koopmann, *Phys. Rev. Lett.* 92, 067009 (2004); T. Giamarchi and S. Bhattacharya, in *High Magnetic Fields: Applications to Condensed Matter Physics and Spectroscopy*, edited by C. Bertier, L. P. Levy and G. Martinez (Springer Verlag, 2002), p. 314, and references therein.
¹⁸ S. S. Banerjee *et al.*, *Phys. Rev. B* 58, 995 (1998); S. S. Banerjee *et al.*, *Physica C* 355, 39 (2001) and references therein.
¹⁹ S. Sarkar *et al.*, *Phys. Rev. B* 61, 12394 (2000); *Phys. Rev. B* 64, 144510 (2001); S. Sarkar *et al.*, *Physica C* 356, 181 (2001); and S. Sarkar, Ph.D. thesis (TIFR), University of Mumbai (2002), India.
²⁰ D. Jaiswal-Nagar *et al.*, *Phys. Rev. B* 74, 184514 (2006).
²¹ C. V. Tomy, G. Balakrishnan, and D. McK. Paul, *Phys. Rev. B* 56, 8346 (1997).
²² C. V. Tomy, G. Balakrishnan, and D. McK. Paul, *Physica C* 280, 1 (1997).
²³ K. Kadowaki, *Physica C* 185, 2249 (1991).
²⁴ P. H. Kes *et al.*, *Phys. Rev. Lett.* 67, 2383 (1991).
²⁵ A. K. Grover *et al.*, *Pramana-J. Phys.* 42, 193 (1994).
²⁶ C. P. Bean, *Phys. Rev. Lett.* 8, 250 (1962); *Rev. Mod. Phys.* 36, 31 (1964).
²⁷ C. V. Tomy, R. Kumar and A. K. Grover, *Solid State Comm. C* 80, 117 (1991).
²⁸ J. Deak *et al.*, *Phys. Rev. B* 47, 8377 (1993); J. Deak *et al.*, *Phys. Rev. B* 49, 6270 (1994).
²⁹ J. Clem and Z. Hao, *Phys. Rev. B* 48, 13774 (1993).
³⁰ A. K. Grover *et al.*, *Physica C* 192, 372 (1992).
³¹ A. K. Grover *et al.*, unpublished.